

Comparative analysis of auction mechanisms and bidding strategies for P2P solar transactive energy markets

Jason Lin^a, Manisa Pipattanasomporn^{a,b}, Saifur Rahman^a

^a Bradley Department of Electrical and Computer Engineering, Advanced Research Institute, Virginia Tech, Arlington, VA, USA

^b Smart Grid Research Unit, Department of Electrical Engineering, Chulalongkorn University, Thailand

HIGHLIGHTS

- A comparative analysis of auction mechanisms and bidding strategies is presented.
- Impacts of bidding strategies & auction mechanisms on various markets is simulated.
- The best-offer game theoretic strategy results in near-ideal economic efficiencies.
- Results show that discriminatory k-DA can economically outperform uniform k-DA.
- However, discriminatory k-DA is more sensitive to market conditions than uniform k-DA.

ARTICLE INFO

Keywords:

Blockchain
Double auction
Game theory
Peer-to-Peer (P2P) energy trading
Smart contracts
Transactive energy

ABSTRACT

The advent of blockchain technology and the increasing penetration of rooftop photovoltaic (PV) systems have presented a new opportunity for peer-to-peer (P2P) energy trading. In such transactive markets, communities may enjoy cheaper electricity prices while supporting locally produced green energy. However, there exists a considerable knowledge gap between market mechanisms and energy exchanges. Challenges arise in the auction process to ensure individual rationality, incentive compatibility, budget balance, and economic efficiency. This paper offers insights for building the foundation of a P2P energy trading market and presents a comparative analysis of auction mechanisms and bidding strategies for P2P solar electricity exchanges in terms of market demand and supply metrics. Auction mechanisms considered in this paper are Discriminatory and Uniform k -Double Auction (k-DA). Impacts of different bidding strategies, including game theoretic approaches, on the economic efficiencies of the P2P transactive energy market are also studied. A simulation case study of 100 participants in a microgrid at various PV penetration levels is presented using typical residential load and solar PV generation profiles.

1. Introduction

Universally, electric grids have been based on a centralized unidirectional system where power flows from large-scale utility generators to customer loads. With the declining price of renewable energy technologies and the institution of green energy policies, electric grids are transforming into a more decentralized system where power may be generated and consumed by prosumers. In the U.S., the 28% decline in installation costs of small-scale photovoltaic (PV) systems from 2014 to 2018 [1] together with the increasing requirements of renewable portfolio standards have led to more than a tripling of their installed capacity from 3.3GW to 11GW in just four years [2]. As of November 2018, there are more than 1.8 million U.S. prosumers supplying power back into the grid [3].

These prosumers are compensated via net metering and alternative programs such as feed-in tariffs [4]. In the U.S., 38 states out of 50 along with Washington, D.C. have mandated net metering rules as of October 2018 [5]. Seven states (Arizona, Georgia, Hawaii, Indiana, Nevada, Maine, Mississippi) have alternate compensation plans, such as feed-in tariffs. Through Michigan's Experimental Advanced Renewable Energy Program, the state mandated utilities to offer residential prosumers a premium feed-in tariff of \$0.24/kWh between 2009 and 2029 [6]. This is nearly double the average retail cost of electricity at \$0.1268/kWh (August 2009) [7]. As the number of prosumers are increasing, certain states are now beginning to phase out net metering rules and premium feed-in tariffs, opting for compensation programs at or near the avoided cost rate [8]. This rate, which is significantly lower than the retail price of electricity, represents the marginal cost for a

E-mail address: jason.lin@vt.edu (J. Lin).

utility to produce one more unit of power. For example, Indiana's Senate Bill 309 planned to phase out net metering by July 2022 [9]. If Indiana's net metering program were terminated in November 2018, homeowners would be billed \$0.1238/kWh for electric consumption while being compensated at \$0.0537/kWh for energy production [10,11].

As penetration of DERs increases and adoption incentives fade, a transactive energy (TE) market may likely emerge [12]. A novel approach to implement such a TE market is through P2P energy trading on blockchain technology [13,14]. P2P energy trading may increase network resilience, provide monetary benefits, allow individuals to exercise purchase decisions on alternative energy sources, and even foster a greater sense of community [15]. Blockchain technology further facilitates P2P energy trading by offering a higher level of trust, fairness, and automation without depending on a central clearinghouse [16,17].

Several P2P energy trading pilots exist as of 2018. In the U.S., residential neighbors in the Brooklyn Microgrid have traded locally produced solar energy [18]. The P2P energy trading network was launched in March 2016 with the system built on smart meters and the Ethereum blockchain [19]. The market cleared every 15 min via sealed-bid double auction with uniform prices [20]. In Australia, the Latrobe Valley Microgrid project started in March 2018 and aims to create a local energy marketplace for dairy farmers, residents, as well as commercial and industrial customers [21]. In Thailand, the T77 precinct in Bangkok is conducting energy trading trials involving apartments, a shopping center, a school, and a dental hospital on the Power Ledger platform [22]. In the UK, the Piclo project hosts online auctions for demand response aggregators, energy suppliers, and vehicle charging operators [23]. The Electron project provides platforms for meter registration and flexible energy trading on blockchain technology [24]. In Germany, the sonnenCommunity expands P2P energy trading with the use of batteries [25]. In Singapore, a decentralized energy marketplace is being built for consumers, commercial energy suppliers, as well as private producers via the Synergy platform [26]. In Spain and Estonia, WePower connects customers with green power producers through digital power purchase agreements [27]. The Share&Charge project provides a decentralized protocol for electric vehicle charging, transactions, and data sharing [28].

Despite the growing number of P2P energy trading projects, there still exist knowledge gaps between how market mechanisms interact with market conditions. One research attempts to close this gap by evaluating P2P energy sharing mechanisms, such as supply and demand ratio (SDR) [29], mid-market rate (MMR) [30] and bill sharing (BS) [30] based on a multi-agent simulation through various economic and technical indexes [31]. However, these mechanisms consider prosumers as price takers. Uniform market clearing prices are determined for both consumers and prosumers based on the supply/demand of electricity and grid retail/feed-in tariff rates; participants do not place competitive bids in an auction-based approach. Another study, which proposes a primal-dual algorithm for double energy auctions, unrealistically assumes that both buyers and sellers aim to lower the overall cost of electricity [32]. Other studies consider motivational psychology and model energy trading as canonical coalition games with price-taking participants [33,34]. A more complex model that realistically describes a free market considers participants as price-makers [35]. In this concept, agents are aware of their own market power and place strategic bids accordingly. Authors in [36] investigate a proportionally fair double-sided energy auction with price anticipating participants. Other studies, however, set participants to always bid their truthful value based on load consumption of specific appliances [37]. Some research focuses on game-theoretic analysis that resemble Cournot competition [38] as well as Stackelberg games [39,40]. Authors in [41] further combine consumer-prosumer energy trading with grid-grid transactions to form a two-tier double auction energy market. Other studies explore effects of battery storage and control within a local P2P energy market

[42,43]. Authors in [44] additionally coordinate demand side management with P2P energy trading, arriving at a near-optimal cost optimization algorithm. While there are many models to describe a P2P energy market [45], appropriate trading mechanisms ultimately rest on government policies and local market conditions and market goals. These contexts thus define the market of interest, such as a free versus regulated market (modeled by price-making or price-taking participants, respectively) that induces social welfare, truthful bidding, balanced budget, and/or individual rationality. These four characteristics are further explained in Section 2.

This paper aims to prepare for the future of DERs by offering insights for building a P2P TE market. While current research has investigated auction design and energy trading, their economic efficiencies and performance in response to different bidding strategies have not been comparatively analyzed. In addition, their operations in terms of varying PV penetration levels within a microgrid have not been particularly investigated. Thus, major contributions of this research include proposing two game-theoretic participant bidding strategies, modeling the behavior of P2P TE markets against different PV penetration levels, comparatively analyzing the economic efficiencies of various auction mechanisms, and investigating the effects of various bidding strategies on market conditions.

2. Review of auction mechanisms and proposed evaluation metrics

In the context of P2P energy trading, auction mechanisms are implemented within smart contracts to match offers from buyers and sellers. This section describes the methodologies involved in selecting and evaluating auction mechanisms for the simulated case studies presented in this paper.

2.1. Review of auction mechanisms

While a multitude of mechanisms exist, commonly known auction mechanisms, such as Discriminatory k -Double Auction (k -DA), Uniform k -DA, Vickrey-Clark-Groves (VCG), and Trade Reduction (TR), are briefly reviewed.

Table 1 summarizes these mechanisms in terms of the trading prices buyers pay and the trading prices sellers receive in any given single-unit transaction.

In Discriminatory k -DA [46], otherwise known as Pay-as-Bid k -Double Auction, buyers submit sealed bid prices B^P while sellers submit sealed ask prices S^P . Following the natural ordering rule, bid prices are sorted in a descending order while ask prices are sorted in an ascending order. If $B^P \geq S^P$, a trade occurs at the listed price in **Table 1** where k is a predetermined constant in the closed interval $[0, 1]$. Since the trading price is determined between each winning buyer-seller pair, the described mechanism is discriminatory. A single market clearing price does not exist for each auction interval.

Uniform k -DA is a variation to discriminatory k -DA where all winning participants trade at the same price. Such market clearing price is figured by first sorting offers according to the natural ordering rule and determining the largest breakeven index γ where $B_\gamma^P \geq S_\gamma^P$. The market clearing price is then calculated as for single-unit auctions where B_γ^P

Table 1
Auction mechanisms.

Auction mechanism	Price trading buyers pay	Price trading sellers receive
Discriminatory k -DA	$kB^P + (1 - k)S^P$	
Uniform k -DA	$kB_\gamma^P + (1 - k)S_\gamma^P$	
VCG	$\max(S_\gamma^P, B_{\gamma+1}^P)$	$\min(S_{\gamma+1}^P, B_\gamma^P)$
TR	B_γ^P	S_γ^P

and S_γ^P are the bid and ask prices at the largest breakeven index, respectively.

The Vickrey-Clark-Groves (VCG) mechanism is an alternative auction mechanism that maximizes social welfare and motivates participants to bid truthfully at the expense of the market operator [46]. $B_{\gamma+1}^P$ and $S_{\gamma+1}^P$ are the bid and ask prices following the largest breakeven index, respectively. Effectively, $B_\gamma^P \geq B_{\gamma+1}^P$ and $S_\gamma^P \leq S_{\gamma+1}^P$ due to the natural ordering rule for sorting offers. Since the price that trading buyers pay is less than the price that trading sellers receive, there exists a deficit that needs to be subsidized by the market operator to facilitate the transaction.

The Trade Reduction (TR) auction mechanism avoids subsidization of trades while maintaining truthful bidding by limiting trades to $\gamma - 1$ buyers and sellers [45]. Such differs from uniform k -DA and VCG, where γ buyers and sellers are allowed to transact. Because buyer γ and seller γ are not permitted to participate in the TR auction, social welfare is not maximized. However, trading buyers pay B_γ^P and trading sellers receive S_γ^P . As $B_\gamma^P \geq S_\gamma^P$, the market operator may financially gain $B_\gamma^P - S_\gamma^P$ from each single unit transaction.

Each of the previously reviewed mechanisms exhibit varying characteristics. An ideal auction mechanism encompasses four distinct properties: individual rationality (IR), budget balance (BB), incentive compatibility (IC), and economic efficiency (EE) [47]. An IR mechanism implies that no buyers/sellers shall result in negative utilities from participating in the auction. All four reviewed mechanisms exhibit IR. A BB mechanism does not financially subsidize or gain from transactions between buyers and sellers. Both VCG and TR are not BB as their market operators financially subsidize and gain from trades, respectively. IC motivates participants to bid their valuations truthfully. Both Discriminatory and Uniform k -DA do not have mechanisms to motivate truthful bidding as VCG and TR do. EE attempts to maximize the sum of all individual utilities for social welfare such that no participants are precluded from trading. Since buyer γ and seller γ are precluded from trading in TR, the mechanism, by default, does not maximize economic efficiency. While an ideal auction mechanism shall exhibit all four properties, it is important to note that the Myerson-Satterthwaite theorem [48] proves that no realistic mechanism can exhibit these four properties simultaneously. Thus, an appropriate trading mechanism for a realistic market rests on the prioritization of these four factors tailored for the context of the local market: should the market allow non-truthful bidding? Should the market attempt to maximize social welfare? Should the market respect individual rationality? Should the market keep transactions budget balanced? While answering these questions is beyond the scope of this study, Table 2 summarizes the properties of the discussed auction mechanisms.

In this study, Discriminatory and Uniform k -DA are selected as the mechanisms of interest to support a simulated TE market as they are the most common auction processes. Known as Double Auction with Average Mechanism when $k = 0.5$, both mechanisms exhibit individual rationality, budget balance, and economic efficiency out of the four properties; only incentive compatibility is lacking. This will thus make an interesting comparison to investigate how discriminatory versus uniform pricing mechanisms interact with and respond to the market.

Table 2
Mechanism properties.

Auction mechanism	IR	BB	IC	EE
Discriminatory k -DA	✓	✓		✓
Uniform k -DA	✓	✓		✓
VCG	✓		✓	✓
TR	✓		✓	

2.2. Proposed evaluation metrics for economic efficiency

Performance evaluation of auction mechanisms can reveal how they respond to market conditions. While all four mechanism properties are predetermined by the formulation of mechanism itself, a mechanism's degree of economic efficiency in response to market conditions can be quantitatively analyzed [49].

We propose three economic efficiency evaluation metrics: percentage of kWh sold, percentage of kWh bought, and percentage of households cleared [48] within the microgrid, as summarized in Table 3.

Table 3
Economic efficiency evaluation metrics.

Metric	Calculation
Percentage of kWh sold (sellers' perspective)	$\sum_{m=1}^{N_T} T_m^Q / \sum_{j=1}^{N_S} S_j^Q$
Percentage of kWh bought (buyers' perspective)	$\sum_{m=1}^{N_T} T_m^Q / \sum_{i=1}^{N_B} B_i^Q$
Percentage of households cleared (market operator's perspective)	$\frac{\sum_{i=1}^{N_B} \left \frac{B_i^{Qfull}}{B_i^Q} \right + \sum_{j=1}^{N_S} \left \frac{S_j^{Qfull}}{S_j^Q} \right }{N_B + N_S}$

Where,

N_B, N_S, N_T	Total number of buyers, sellers, and trades
B_i^Q	kWh quantity demanded by buyer i
S_j^Q	kWh quantity supplied by seller j
B_i^{Qfull}	Cleared kWh quantity for buyer i ; $\leq B_i^Q$
S_j^{Qfull}	Cleared kWh quantity for seller j ; $\leq S_j^Q$
T_m^Q	Total kWh quantity transacted for trade m

The first two metrics represent the percentage of successfully traded commodities within the microgrid from the perspectives of sellers and buyers, respectively. A P2P market with higher percentage of kWh sold would attract sellers to participate. Similarly, a P2P market with higher percentage of kWh bought would encourage participation from buyers. From the market operator's perspective, the percentage of households cleared is defined as the ratio of participants whose orders have been completely fulfilled to the total number of participants. A higher percentage of households cleared implies higher fulfilment of a community's energy needs and surplus – thus, better market operation. These metrics are calculated at each hourly auction interval and averaged for the duration of excess solar energy generation.

3. Proposed game-theoretic bidding strategies

In this study, a double auction is of interest so that both buyers and sellers may submit bids to trade excess solar electricity. Offers from both buyers and sellers consist of bid/ask prices as well as quantity in kWh. These bid/ask prices are determined based on the proposed game-theoretic approaches, where the game is non-cooperative, non-zero-sum, and simultaneous-move. All agents strategically attempt to maximize self-interests; all agents submit sealed bids without knowledge of the actions of other players.

For simplicity, a two-player game is considered where an individual buyer bids against all other buyers while an individual seller bids against all other sellers. Each participant has three strategies: to bid lower, same, or higher than the previous-hour market price. The degree of bidding deviation from the previous-hour market rate is determined by each agent's low and high preferences. These two preference factors for participant i (i.e., $\delta_i^{strategy}$) are generated via sampling a normal distribution with a mean of 0 and a standard deviation of 0.15. The low

preference factor is constrained to a negative value while the high preference factor is constrained to a positive value. Participant i can thus place a potential bid/ask price (i.e., χ_i^{strategy}) of:

$$\chi_i^{\text{strategy}} = P_{\text{seed}} * (1 + \delta_i^{\text{strategy}}) \quad (1)$$

where P_{seed} is the seed price (\$/kWh) from the previous-hour market rate and $\delta_i^{\text{strategy}}$ is the preference factor for participant i adopting a low/same/high strategy. Similarly, since the game is modeled as simultaneous-move with sealed bids, participant i would anticipate the potential bid/ask price of all other buyers/sellers for each strategy (i.e., $\chi_{\text{others}}^{\text{strategy}}$) by predicting their preference factors (i.e., $\delta_{\text{others}}^{\text{strategy}}$) over the previous-hour market rate.

In turn, the utility in \$/kWh for participant i can be defined as $U_i^{\text{strategy}} = \zeta_i - \chi_i^{\text{strategy}}$ for buyers and $U_i^{\text{strategy}} = \chi_i^{\text{strategy}} - \zeta_i$ for sellers, where ζ_i is the cost (\$/kWh) to participant i , given below:

$$\zeta_i = \begin{cases} P_{\text{retail}} & \text{if participant } i \text{ is a buyer} \\ \frac{P_{\text{install}}}{\tau^* \lambda} & \text{if participant } i \text{ is a seller} \end{cases} \quad (2)$$

The buyer's "marginal cost" is assumed to be the average retail cost of electricity from the utility company. This represents the cost to acquire an additional kWh (\$/kWh) from the electric utility. The buyer may thus gain a high utility when there exists a high differential between the cost of electricity from the utility company and the P2P energy trading network.

On the other hand, the seller's "levelized cost" is the cost to generate an additional kWh of electricity (\$/kWh) over the useful life of their installed PV system. This is defined as the ratio of total installed PV system cost (\$), including operation and maintenance costs, to the estimated generation (kWh) over its useful life of 20 years. This simplified model does not consider degradation of PV panels over time. In this study, total installed PV system cost for each prosumer is calculated by:

$$P_{\text{install}} = P_{\text{est}} * A_{\text{roof}} * \alpha * W_{\text{PV}} / A_{\text{PV}} \quad (3)$$

where P_{est} is the system cost per watt (\$/W), including annualized operation and maintenance costs, randomly generated from the closed interval [3.00, 4.50] [50]; A_{roof} is the one-sided area of the gable roof in square feet; α is the percentage of usable roof space for PV panel installation, assumed to be 70% [51]; W_{PV} is the size of the installed PV panels in watts; and A_{PV} is the area of the installed PV panels in square feet.

With all necessary information defined and utilities calculated, the normal-form game can be constructed by each participant as illustrated in Table 4. In reality, participation into such market by each buyer and

Table 4
Normal-form game.

All Other Buyers/Sellers			
	$\chi_{\text{others}}^{\text{lower}}$	$\chi_{\text{others}}^{\text{same}}$	$\chi_{\text{others}}^{\text{higher}}$
χ_i^{lower}	$\pi_i^{\text{lower}}, \pi_{\text{others}}^{\text{lower}}$	$\pi_i^{\text{lower}}, \pi_{\text{others}}^{\text{same}}$	$\pi_i^{\text{lower}}, \pi_{\text{others}}^{\text{higher}}$
χ_i^{same}	$\pi_i^{\text{same}}, \pi_{\text{others}}^{\text{lower}}$	$\pi_i^{\text{same}}, \pi_{\text{others}}^{\text{same}}$	$\pi_i^{\text{same}}, \pi_{\text{others}}^{\text{higher}}$
χ_i^{higher}	$\pi_i^{\text{higher}}, \pi_{\text{others}}^{\text{lower}}$	$\pi_i^{\text{higher}}, \pi_{\text{others}}^{\text{same}}$	$\pi_i^{\text{higher}}, \pi_{\text{others}}^{\text{higher}}$

seller will reply on a software agent that calculates payoffs and automatically chooses the best bidding strategy based on available information.

Where π_i^{strategy} represents the payoff of participant i when the corresponding strategy is chosen. This study establishes two payoff determination methods which are further described in Sections 3.1 and 3.2: best-offer approach and market-power approach, respectively. The payoff determination method decides whether participant i or the collective of all other buyers/sellers get their utilities when comparing potential bid/ask prices for each of their potential strategies.

Once the payoff matrices are constructed for each buyer and seller, each party determines their own dominant strategy – the strategy that results in the highest payoff regardless of the opponent's strategy. This represents a Nash Equilibrium, where given the strategies of other players, no player can improve his payoff by changing his own strategy. If multiple or no Nash Equilibrium exists, players adopt mixed strategies and randomly select a strategy within the solution space.

3.1. Best-offer approach

In the best-offer approach, participants compete to bid for the best price and do not take into consideration market supply and demand for excess PV energy.

Thus, when participant i is a seller, their payoff can be determined by:

$$\pi_i^{\text{strategy}} = \begin{cases} U_i^{\text{strategy}} & \text{if } \chi_i^{\text{strategy}} < \chi_{\text{others}}^{\text{strategy}} \\ 0 & \text{otherwise} \end{cases} \quad (4)$$

$$\pi_{\text{others}}^{\text{strategy}} = \begin{cases} U_{\text{others}}^{\text{strategy}} & \text{if } \chi_{\text{others}}^{\text{strategy}} \leq \chi_i^{\text{strategy}} \\ 0 & \text{otherwise} \end{cases} \quad (5)$$

Due to the natural ordering rule, an individual seller must bid lower than all other sellers in order to win a non-zero payoff. In other words, a seller with a lower ask price gets to clear its bid before sellers with higher ask prices. In contrast, the collective of "all other sellers" may bid equal to participant i to win a non-zero payoff. Because the collective has a greater number of sellers, it is assumed that they have a higher possibility of winning the bid than the individual seller.

When participant i is a buyer, their payoff can be determined by:

$$\pi_i^{\text{strategy}} = \begin{cases} U_i^{\text{strategy}} & \text{if } \chi_i^{\text{strategy}} > \chi_{\text{others}}^{\text{strategy}} \\ 0 & \text{otherwise} \end{cases} \quad (6)$$

$$\pi_{\text{others}}^{\text{strategy}} = \begin{cases} U_{\text{others}}^{\text{strategy}} & \text{if } \chi_{\text{others}}^{\text{strategy}} \geq \chi_i^{\text{strategy}} \\ 0 & \text{otherwise} \end{cases} \quad (7)$$

In the same way, an individual buyer must bid higher than all other buyers in order to win a non-zero payoff; the collective of "all other buyers" must bid at least equal to participant i to win a non-zero payoff. Such describes a "winner-takes-all" situation because the losing party gets a zero payoff.

3.2. Market-power approach

With the knowledge of market conditions such as historical data of total PV generation and total electrical demand of the microgrid, different payoff matrices can be formulated for buyers and sellers. For example, when $\text{demand} > \text{supply}$ is projected for the next hourly interval, a sellers' market results. Competition among buyers to place winning bids is high. Thus, buyers employ the above best-offer payoff logic in an effort to bid the highest price. However, prosumers need not compete as intensely with other prosumers due to a predicted sellers' market. Thus, the payoff determination logic for sellers is:

$$\pi_i^{\text{strategy}} = U_i^{\text{strategy}} \quad (8)$$

$$\pi_{\text{others}}^{\text{strategy}} = U_{\text{others}}^{\text{strategy}} \quad (9)$$

In this situation, both the individual seller and the collective of “all other sellers” have non-zero payoffs without any imposed conditions. Such win-win situation presumes that the limited supply of excess PV energy will be totally consumed by buyers. Thus, sellers may maintain their prices without losing bids when competing against all other sellers.

In order to assess the formulated game-theoretic bidding strategies, we compare the two payoff determination methods with the following participant bidding behaviors in the case study presented in Section 4.

Random (Uniform Distribution): This assumes that each consumer/prosumer bids at a random bid/ask price without any strategic anticipation and disregards the historical and market retail costs of electricity. Bid/ask prices are randomly sampled from a uniform distribution inclusively between \$0.01/kWh and \$1.00/kWh.

Preference Factor: This resembles a household’s preference to always submit offers more/less than the previous-hour market rate. Thus, bid/ask prices are generated from a discount/markup factor of the previous-hour market price. This behavior is modeled via sampling a normal distribution with a mean of 0.2 and standard deviation of 0.15 to assume that most buyers seek a 20% discount from market rates and most sellers seek a 20% premium from market rates. While there does not seem to be an area of intersection for matched buyer and seller offers, such accounts for situations where a small portion of consumers are willing to pay more for locally produced green energy and a small portion of prosumers are willing to sell at a lower price for the benefit of the community.

Since discriminatory auction mechanisms do not have a uniform market clearing price at each auction interval, the historical market price is determined by the weighted average of all transactions during the interval:

$$P_{\text{seed}} = \frac{\sum_{m=1}^{N_T} T_m^Q * T_m^P}{\sum_{m=1}^{N_T} T_m^Q} \quad (10)$$

Because P_{seed} is not available for the first auction interval, it is set as the average of $P_{\text{wholesale}}$, the wholesale/avoided cost of electricity, and P_{retail} , the average retail cost of electricity, in a specified locality.

4. Case study description

This study targets a hypothetical microgrid of 100 homes located in the Washington, D.C. metropolitan area. Microgrid description and simulation scenarios are discussed below.

4.1. Microgrid description

House sizes: Typical house sizes in this region range from 1,000 to 4,000 square feet, and are either single-story or two-stories tall. To simulate this microgrid, a uniform distribution of house sizes was randomly generated from the aforementioned ranges.

Load profiles: The hourly base load profile for a typical house in the Washington, D.C. metropolitan area was obtained from the Building America Housing Simulation B10 Benchmark [52]. Shown in Fig. 1, the base load profile represents the electrical consumption (kW) of an average house size of 2,546 square feet during a summer month. The load profile of each house in the microgrid was determined by scaling the base load profile proportionally to the previously generated home size. Additionally, a random $\pm 20\%$ deviation is introduced in each home’s load profile to induce variability.

PV generation profiles: The hourly base PV generation profile was derived from a 6.44 kW PV system of 485 square feet installed at a Virginia Tech research facility in Arlington, Virginia, USA. Shown in

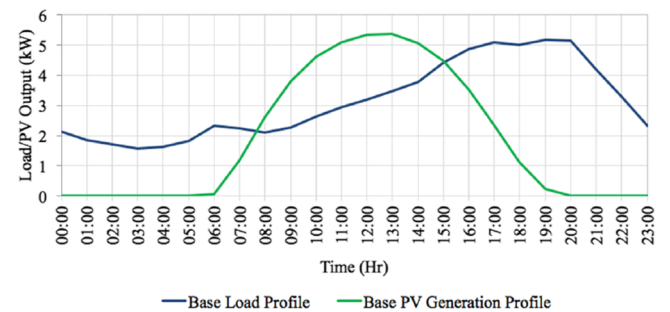


Fig. 1. A 24-hr base load and PV generation profile.

Fig. 1, the base PV generation profile represents the electrical generation (kW) from this PV system on a sunny day during a summer month.

The PV generation profile for each prosumer was determined by scaling the base PV generation profile to the size of usable roof space of each home. All homes are assumed to have gable roofs (Fig. 2) with only 70% of one side utilized for PV installation [50,53]. Conventional roof pitches (slopes) for residential homes range from $\tan\theta = [4/12, 9/12]$ [54]. Through reverse area projection, the one-sided roof area (A_{roof}) can be derived from the house foundation area ($A_{\text{foundation}}$) by $A_{\text{roof}} = 0.5A_{\text{foundation}}\cos^{-1}\theta$. A random $\pm 20\%$ deviation was also introduced to the PV generation profile to account for variations in efficiency, tree shading, cloud coverage, etc.

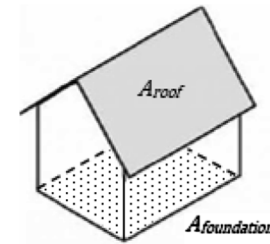


Fig. 2. Gable roof.

Average retail cost of electricity: The average retail cost of electricity in this locality is \$0.1234/kWh and the average wholesale rate of electricity is \$0.033/kWh [10]. The average of these two prices is used as the seed price (P_{seed}) for preference factor and game theoretic bidding strategies.

4.2. Simulation scenarios

Fig. 3 summarizes the various scenarios that are studied. For a microgrid of 100 homes, three PV penetration levels are tested (30%, 50%, 70%) with four participant bidding strategies (random, preference factor, best-offer game theory, and market-power game theory). Offer prices from all participants are sorted by price according to the natural ordering rule. Both discriminatory and uniform k -DA mechanisms are tested with three degrees of k values: 0, 0.5, and 1. These scenarios are simulated using a custom simulation framework developed by the author to model the high-level behavior of the P2P energy trading market. The framework allows any number of defined auction mechanisms, ordering rules, bidding strategies, number of houses in a microgrid, as well as buyer/seller ratios to be simulated. Additionally, the simulation framework supports arbitrary duration datasets for load and PV generation profiles.

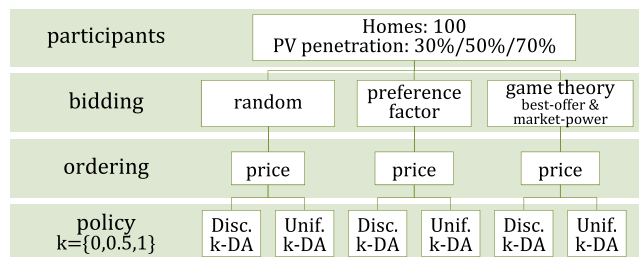


Fig. 3. Simulated scenarios.

5. Results and observations

Results are discussed below based on PV penetration levels of the microgrid. For each PV penetration scenario, impacts of different auction mechanisms and bidding strategies on economic efficiency metrics are investigated.

5.1. Case I: 30% PV penetration

Fig. 4 represents the 24-hour load and PV output profiles for a microgrid of 70 consumers and 30 prosumers. Note that the load profile for the 70 consumers is stacked on top of the aggregate load profile for the 30 prosumers. The summation of these two profiles indicate total load of the microgrid. Due to a 30% prosumer to consumer ratio, total prosumer load is lower than the total consumer load. As shown, the peak load of this microgrid is ~500 kW between the hours of 17:00 and 20:00. The total PV capacity in this scenario is 263.9 kW; peak PV output is ~200 kW from 11:00 to 14:00. There is excess solar energy production from the prosumers between ~07:30 to 16:00 that can be traded among neighbors within the microgrid.

In this scenario consisting of 30% prosumers, the ideal market performance shown in Fig. 5 would result regardless of auction me-

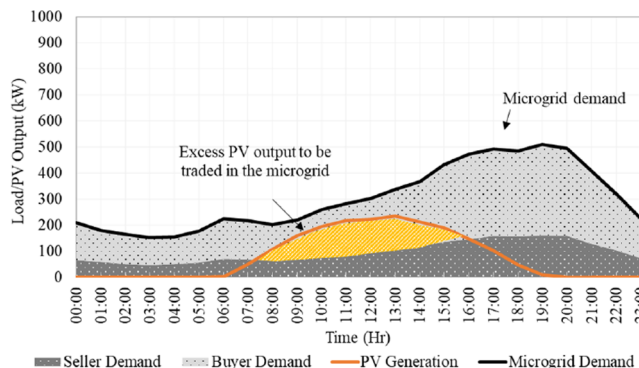


Fig. 4. Microgrid supply vs demand at 30% PV penetration level.

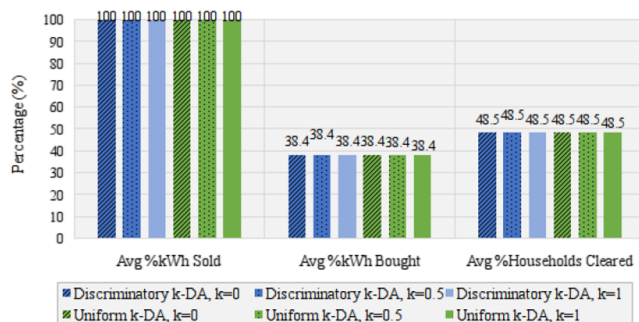


Fig. 5. Ideal market performance at 30% PV penetration.

chanisms if all participants bid exactly the same price. Such is valid as only quantities supplied and demanded are taken into account. Thus, the average percentage of kWh sold is 100% because all excess generated PV energy can be consumed by buyer demand. The average percentage of kWh bought is 38.4% as this is the ratio between excess PV output (yellow shaded area in Fig. 4) and buyer demand (light-gray shaded area) for the duration of excess PV generation. At 30% PV penetration, this ideal scenario can completely fulfill orders of, on average, 48.5% of all households in the microgrid.

Fig. 6(a)–(d) summarizes the market performance at 30% PV penetration in terms of discriminatory k-DA and uniform k-DA when different bidding strategies are employed, as explained below.

5.1.1. Random bidding strategy

When bidding prices are determined at random, results in Fig. 6(a) indicate that discriminatory k-DA offers the same average percentage of kWh sold/bought and households cleared as those of uniform k-DA. This indicates that discriminatory k-DA is able to fulfill the same amount of orders in the market as uniform k-DA when bid/ask prices/quantities are unchanged throughout the variation of k values. Varying degrees of k values do not affect trading outcomes for discriminatory k-DA nor for uniform k-DA. This makes sense as the condition $B^P \geq S^P$ must occur in both discriminatory and uniform k-DA for respective participants to trade; the k value only affects the trading price between winning buyers and sellers, indicated in Table 1. Thus, both auction mechanisms result in the same number of trading participants and economic efficiencies.

5.1.2. Preference factor bidding strategy

Results of participants employing the preference factor bidding strategy are shown in Fig. 6(b). As expected, the average percentage of households cleared, which indicates the average percentage of fulfilled market orders, is extremely low. This is expected as most sellers submit bids higher than the market rate while most buyers submit bids lower than the market rate. Recall the k-DA mechanism and the property of individual rationality, the conditions $p \leq B^P$ and $p \geq S^P$ must exist for a trade to occur. Thus, the non-zero results in Fig. 6(b) are contributed by buyers or sellers whose preference factors are less than 0. These buyers and sellers do not seek discounts and premiums from market rates, respectively. Instead, these buyers are willing to pay more for locally generated green energy and these sellers are willing to gain less from market rates. These participants represent households whose preferences are to support the local community as well as green energy production.

5.1.3. Best-offer game-theoretic bidding strategy

Results in Fig. 6(c) compare the two k-DA auction mechanisms when participants bid using game theory with best-offer payoff logic. In contrast to Case I scenario 1 (random bidding strategy, 30% PV penetration) where the performance of discriminatory k-DA is maintained regardless of k value, performance under the game-theoretic approach changes with varying k values. Such is expected as the implementation depends on previous-hour market rates while the random bidding strategy does not.

Bidding with the best-offer game-theoretic strategy is nearly ideal in a microgrid with 30% PV penetration. The implementation attempts to optimize each participant's bid price among their peers: buyers attempt to bid the highest price over all other buyers; sellers attempt to bid the lowest price over all other sellers. Because market supply and demand are not considered in the bid price determination process, this results in high economic efficiency as all participants try to offer accommodating prices.

5.1.4. Market-power game-theoretic bidding strategy

Despite results of Case I scenario 3 (best-offer game-theoretic approach, 30% PV penetration) being near-ideal, results of bidding with the market-power payoff logic as shown in Fig. 6(d) are far from ideal.

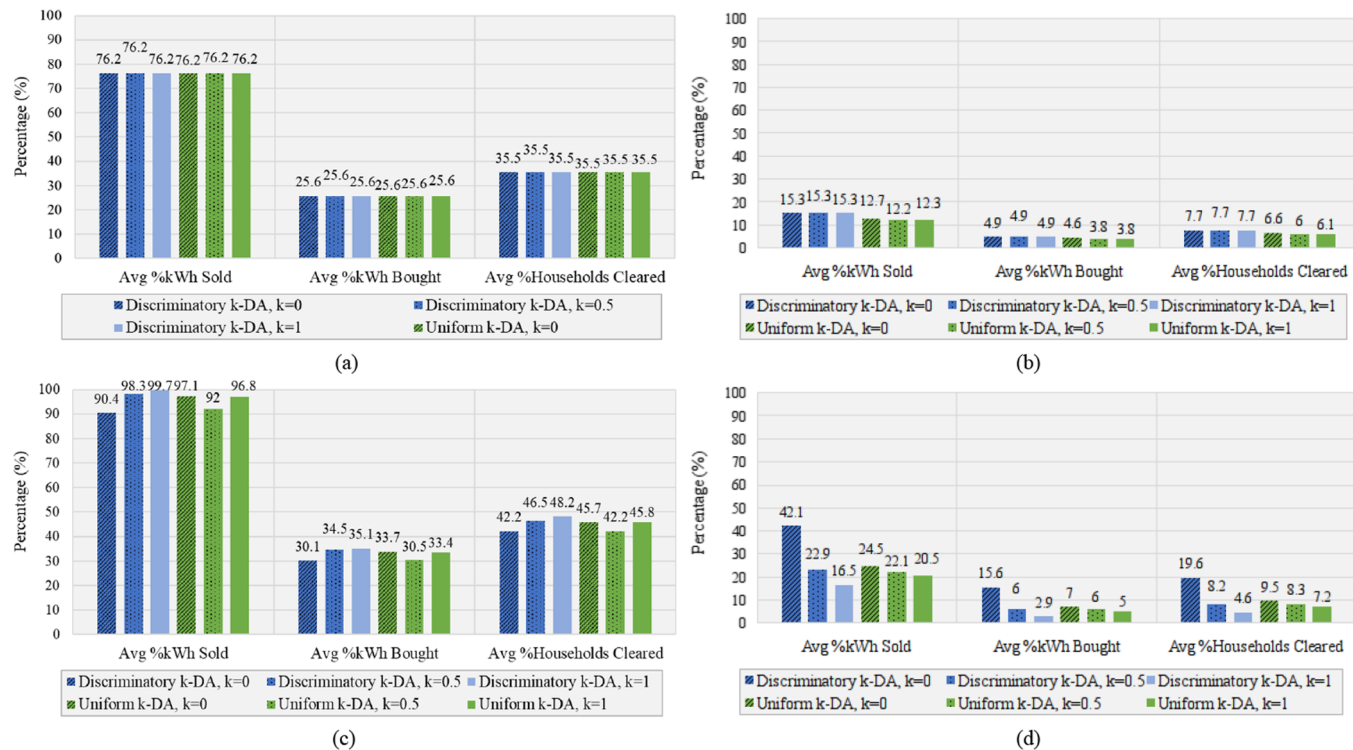


Fig. 6. Performance comparison at 30% PV penetration for (a) random bidding strategy; (b) preference factor bidding strategy; (c) best-offer game-theoretic bidding strategy; and (d) market-power game-theoretic bidding strategy.

Such can be attributed to the high asking prices from the prosumers as there is greater demand than supply. This leads to high market rates and low transaction volumes. Also evident is the increase of market rates as k increases. In turn, fewer participants are able to “clear” market rates. As such, market price for certain mid-day auction periods are null – due to no transaction volume. This explains why there is a downward trend in performance as k increases.

5.2. Case II: 50% PV penetration

Fig. 7 shows the load and PV generation profiles for the microgrid at 50% PV penetration. The total prosumer load approximately mirrors the total consumer load due to the 50/50 seller/buyer ratio. The total PV capacity in this scenario is 456.4 kW; peak PV output is around 390 kW at around 13:00. Similar to Case I, excess solar power is available for trade from ~07:30 to 16:00. Due to a higher PV penetration, there is an excess of PV output between ~08:30 to ~13:30 from the microgrid even after satisfying the microgrid’s demand. The total microgrid demand profile is exactly identical to that of Case I, ensuring fair comparison between tested scenarios.

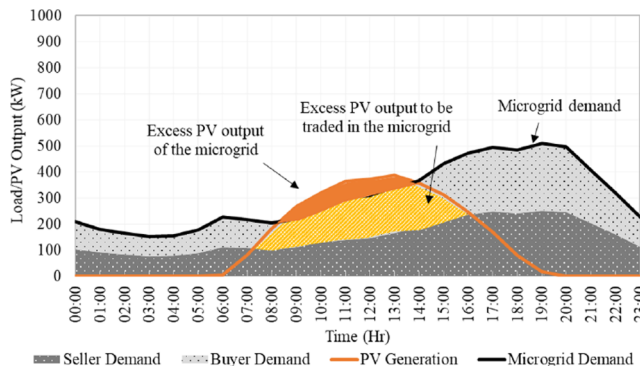


Fig. 7. Microgrid supply vs demand at 50% PV penetration.

Fig. 8 shows the ideal market performance at 50% PV penetration when all participants bid the same price. Note that the average percentage of kWh sold decreased from 100% in the ideal 30% PV penetration scenario to 88.4% due to excess PV output from the microgrid. There is a surplus of supply – thus only 88.4% can be sold within the microgrid to fulfill buyer demand. Due to excess supply and less buyer demand, fulfillment of buyer demand increased from 38.4% to 66.6%. At 50% PV penetration, this ideal scenario can completely satisfy energy needs of, on average, 67.1% of all households in the microgrid.

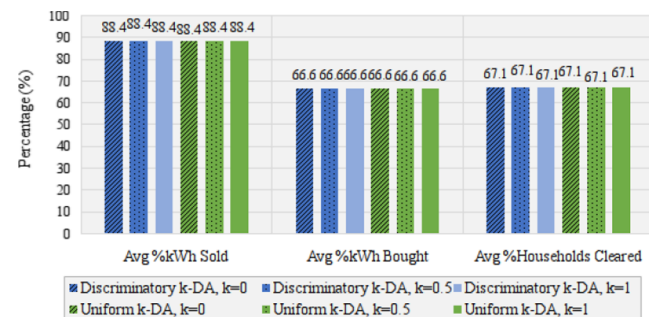


Fig. 8. Ideal market performance at 50% PV penetration.

Fig. 9(a)–(d) summarizes the market performance at 50% PV penetration in terms of discriminatory k-DA and uniform k-DA when different bidding strategies are employed, as explained below.

5.2.1. Random bidding strategy

Results in Fig. 9(a) with participants employing the random bidding strategy in a 50-prosumer microgrid indicate the same generality as a 30-prosumer microgrid (Case I) with participants employing the same strategy. Discriminatory k-DA leads to the same average percentage of households whose orders are completely filled as uniform k-DA. Similarly, all three metrics indicate same results for both mechanisms

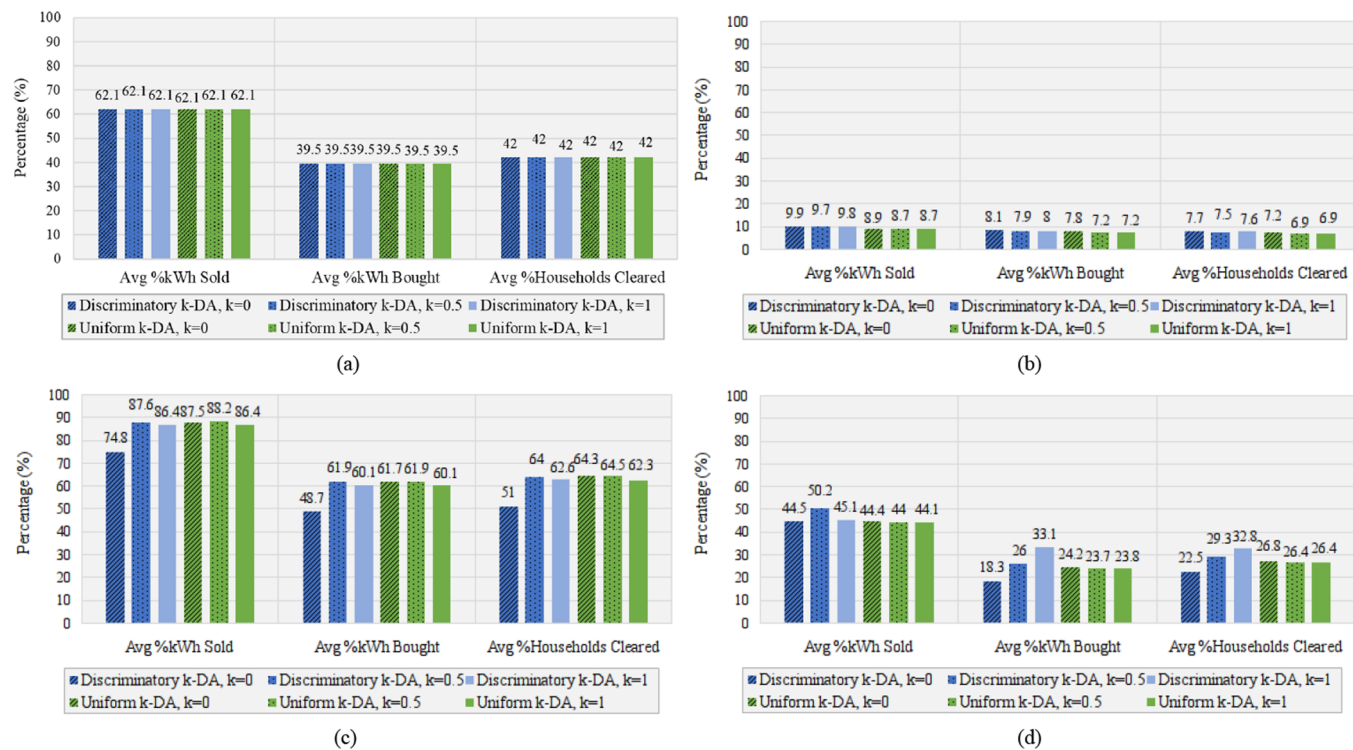


Fig. 9. Performance comparison at 50% PV penetration for (a) random bidding strategy; (b) preference factor bidding strategy; (c) best-offer game-theoretic bidding strategy; and (d) market-power game-theoretic bidding strategy.

regardless of k values. However, there is less average percentage of kWh sold when compared to the 76.2% in Case I scenario 1 (random bidding strategy, 30% PV penetration). This is due to the market having excess supply, more than enough to fulfill microgrid demands in the hours of ~08:30 to ~13:30. In turn, there is a higher percentage of kWh bought because there is no longer a shortage of supply as in Case I scenario 1.

5.2.2. Preference factor bidding strategy

In line with Case I scenario 2 (preference factor bidding strategy at 30% PV penetration), results in Fig. 9(b) show significantly lower performance when compared to other bidding strategies at the same level of PV penetration. In addition, the trend of decreasing average percentage of kWh sold and increasing average percentage of kWh bought follow that of random bidding strategy. This is again due to the microgrid having excess PV supply; there is no longer a shortage of supply as in Case I 30% PV penetration scenarios.

5.2.3. Best-offer game-theoretic bidding strategy

Fig. 9(c) shows the performance when participants employ the best-offer game-theoretic approach in a microgrid with 50% PV penetration. Results reveal that the performance of this bidding strategy is again close to ideal (Fig. 8). Economic efficiencies are comparable for both auction mechanisms with the exception of discriminatory k-DA when $k = 0$. Such can be attributed to low transaction volumes in this scenario.

5.2.4. Market-power game-theoretic bidding strategy

Fig. 9(d) shows the performance of the game-theoretic strategy when a market-power method is used to determine payoffs. There is no longer a decreasing trend in performance as k value increases due to excess supply in the microgrid. Thus at 50% PV penetration, the microgrid is a buyers' market. Such is evident when comparing historical market prices at 30% and 50% PV penetration: market prices for each hour decreased regardless of the auction mechanism. In addition, it can be observed that market rates decrease during the hours of excess

supply (from ~08:30 to ~13:30 as shown in Fig. 7). However outside of those hours when there is more demand than supply, market rates increase.

5.3. Case III: 70% PV penetration

Fig. 10 illustrates the load and PV generation profiles for a microgrid of 30 consumers and 70 prosumers. At 70% PV penetration, the total PV capacity in this microgrid is 640.9 kW; peak PV output is ~530 kW at around 12:00. As in Case II, there is an excess of PV energy from the microgrid between ~07:30 to 15:00 even after self-consumption. Note that there is more demand from the sellers due to higher ratio of prosumers to consumers. However, the total microgrid demand profile maintains the same and is consistent with that of Case I and Case II.

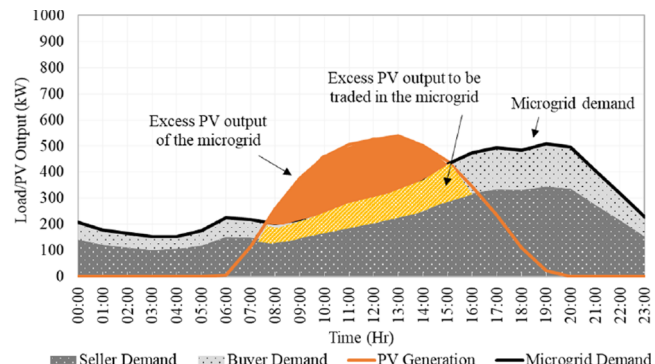


Fig. 10. Microgrid supply vs demand at 70% PV penetration.

Fig. 11 shows the ideal market performance at 70% PV penetration. Average percentage of kWh sold further decreased from Case II (88.4% to 58.5%) due to even more excess PV output from the microgrid. Average percentage of kWh bought increased from 66.6% to 76.7% due



Fig. 11. Ideal market performance at 70% PV penetration.

to less total buyer demand. At 70% PV penetration, this ideal market scenario can completely satisfy energy needs of, on average, 48.9% of all households in the microgrid. This decrease from Case II (67.1% to 48.9%) can be attributed to the higher number of prosumers who are not able to completely sell their excess energy within the microgrid.

The three economic efficiency metrics at 70% PV penetration when different bidding strategies (and auction mechanisms) are implemented is summarized in Fig. 12(a)–(d), as explained below.

5.3.1. Random bidding strategy

Results in Fig. 12(a) indicate the same outcome pertaining to discriminatory and uniform k -DA as in Cases I and II. In line with more excess PV generation, there is a lower average percentage of kWh sold. However, there is a higher average percentage of kWh bought as there is less consumer demand with excess supply. For all three levels of PV penetration with agents employing random bidding strategies, discriminatory k -DA performs equivalently as uniform k -DA with respect to the three defined economic efficiency indices.

5.3.2. Preference factor bidding strategy

Fig. 12(b) presents the trading performance result at 70% PV penetration. The average percentage of kWh sold is the lowest among the



(a)



(c)

three PV penetration scenarios. Such result is consistent with the two other bidding strategies – there is more excess supply from prosumers to meet decreasing consumer load demands. Despite so, the preference factor bidding strategy still results in the lowest performing bidding strategy as most buyers seek a discount from market rates while most buyers seek a premium from market rates. Thus, transactions presented in Fig. 12(b) result from participants who are willing to sacrifice maximization of personal financial gain to support green energy production as well as the local community.

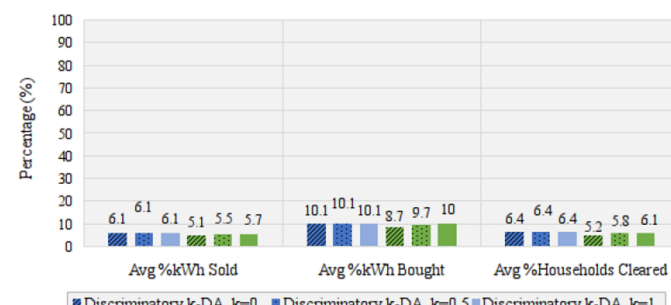
5.3.3. Best-offer game-theoretic bidding strategy

Fig. 12(c) shows the performance comparison for the best-offer game at 70% PV penetration. Once again, performance is near ideal (Fig. 11). With this approach, the amount of transactions between prosumers and consumers is significantly higher than that of the preference factor bidding strategy or random bidding strategy, regardless of the level of PV penetration. In addition, the overall performance of discriminatory k -DA is comparable to that uniform k -DA, regardless of k value.

5.3.4. Market-power game-theoretic bidding strategy

Exhibited in Fig. 12(d), the market-power payoff approach results in significantly worse economic efficiencies than Case II scenario 4 (market-power game, 50% PV penetration). At 70% PV penetration, there is more supply than demand. This scenario is thus a buyers' market, where the low performance can be attributed to buyers who maintain low bids. The effect is further compounded by the k value in the discriminatory mechanism. With even more excess supply than 50% PV penetration, market prices for each hour are observed to have decreased regardless of auction mechanism. Similar to Case II scenario 4 (market-power game, 50% PV penetration), it can be observed that market rates decrease during the hours of excess supply (from ~07:30 to 15:00 in Fig. 10). However outside of those hours when there is more demand than supply, market rates increase.

Regardless of PV penetration and auction mechanism, it is clear that the best-offer game-theoretic bidding strategy results in near-ideal



(b)



(d)

Fig. 12. Performance comparison at 70% PV penetration for (a) random bidding strategy; (b) preference factor bidding strategy; (c) best-offer game-theoretic bidding strategy; and (d) market-power game-theoretic bidding strategy.

performance for all three metrics: average percentage of kWh sold/bought and average percentage of households cleared. However, when supply and demand are considered during the price determination process, performance drops significantly regardless of PV penetration or auction mechanism. Additionally, it can be observed that discriminatory k -DA is more sensitive to market conditions and level of PV penetration, even though it may perform better than uniform k -DA depending on its k value.

6. Discussion

Considered in this study are extreme scenarios where all participants within a microgrid place bids using the same strategies. In a realistic market, participants would employ different strategies, thus leading to results that lie within the findings presented in this paper. However, it is evident that the preference factor bidding strategy results in the lowest performance as participants are modeled to seek personal gain solely from previous-hour market rates without other considerations. Bidding with the market-power game-theoretic approach results in slightly better performance due to participants considering the best strategy to outbid other participants. However, because market supply and demand are considered, buyers from a buyers' market and sellers from a sellers' market may maintain their low and high bids/asks, respectively. Surprisingly, this results in lower performance in contrast to all participants bidding at uniformly random prices. Still, the best performing strategy is the best-offer game-theoretic strategy. This approach results in near-ideal performance in supplying consumer energy needs, selling excess prosumer energy generation, and fulfilling orders within the microgrid market.

The second observation pertains to the economic efficiency of the market-power game-theoretic bidding strategy across various PV penetration levels. From the progression of 30% PV penetration to 50% PV penetration, all other bidding strategies resulted in lower average percentage of kWh sold and higher average percentage of kWh bought within the microgrid. Such follows the same trend in ideal situations where all participants bid at the same price. However, for the market-power game, economic efficiencies increased for both average percentage of kWh sold and average percentage of kWh bought. Additionally, from the progression of 50% PV penetration to 70% PV penetration, all other bidding strategies resulted in even lower average percentage of kWh sold and higher average percentage of kWh bought within the microgrid. However, performance of the two respective metrics decreased for the market-power game-theoretic bidding strategy. Such peculiar behavior is attributed to the participants' knowledge of market supply and demand. Economic efficiencies no longer depend on bid/ask prices, but also on quantities available/needed in the market. Table 5 summarizes the market information for the market-power game for discriminatory k -DA when $k = 0$ and $P_{seed} = 7.82\text{¢}/\text{kWh}$. Clearly, 50% PV penetration results in the highest average percentage of fulfilled

market orders within the microgrid. Such occurs because market supply is more closely matched with market demand than any other PV penetration levels.

Table 5

Market data for market-power game (discriminatory k -DA, $k = 0$, $P_{seed} = 7.82\text{¢}/\text{kWh}$).

PV penetration	30%	50%	70%
Avg %Households Cleared	19.6%	22.5%	11.3%
Traded kWh	268.1	396.9	237.0
Supplied kWh	819.9	1393.2	1957.3
Demanded kWh	2677.9	1914.6	1168.1
Average Market Price	11.01¢/kWh	7.34¢/kWh	6.29¢/kWh

The reflected candlestick charts of hourly market prices for the different levels of PV penetration are shown in Fig. 13. At 30% PV penetration, demand is always greater than supply. Thus, market prices rise. At 50% PV penetration, market rates fall when there is excess supply and rise when there is greater demand in early morning and afternoon. At 70% PV penetration, market rates fall even further during the period of excess PV output from the microgrid.

Additionally, an intriguing phenomenon can be observed in the best-offer game: consistent throughout all three PV penetration levels, the lowest economic efficiency results when $k = 0$. Logically, such occurrence is attributed to the low number of transactions due to a mismatch between buyer bids and seller asks. Upon further investigation of historical market prices, an interesting connection is revealed: all market rates fall within the lower and upper quartiles of the sellers' leveled costs (\$0.0679/kWh and \$0.0841/kWh, respectively). Consequently, the number of transactions decreases as market rates approach leveled costs. Such also explains why certain hours of the market-power game at 30% PV penetration when $k = 1$ resulted in zero trades; market rates quickly approach the mean of the buyers' marginal cost – \$0.1234/kWh.

7. Conclusion and future work

A comparative analysis of auction mechanisms that facilitate a transactive energy market is explored under three levels of PV penetrations. A microgrid of 100 homes at 30%, 50%, and 70% PV penetration levels is simulated through a custom developed framework against four participant bidding strategies and two auction mechanisms. Key findings indicate that regardless of PV penetration and employed bidding strategies, discriminatory k -DA can outperform uniform k -DA in all three performance metrics – average percentage of kWh sold, average percentage of kWh bought, and average percentage of households cleared. Despite so, discriminatory k -DA is more sensitive to market conditions and leads to greater variations in market prices than

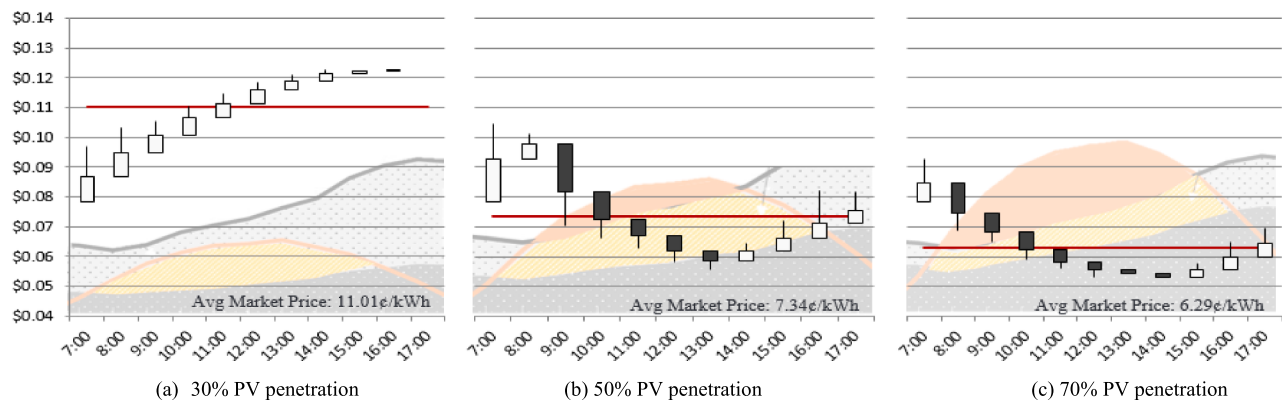


Fig. 13. Comparison of hourly market rates with the market-power game-theoretic bidding strategy (discriminatory k -DA, $k = 0$, $P_{seed} = 7.82\text{¢}/\text{kWh}$).

uniform k-DA.

When participants employ the preference factor bidding strategy, performance with respect to all three metrics is the lowest of the four strategies regardless of implemented auction mechanisms. Such makes sense as the strategy models participant behavior to seek prices better than the previous-hour market rate. In this situation, sellers tend to seek higher returns than the market price while buyers tend to seek lower costs than the market price. If all participants seek better-than-market rates, there would be no transactions within the microgrid. However, such is not the case in a realistic market as some participants may be willing to transact at slightly inferior rates to benefit the local community and support the production of green energy. Bidding with the market-power game-theoretic method results in a slightly higher performance due to participants attempting to outbid other participants rather than focusing on individual gains. Despite so, this strategy underperforms by a significant margin when compared to bidding at uniformly random prices. The best performing strategy is the best-offer game theoretic approach. This method results in near-ideal economic efficiency with respect to all three metrics. Such is due to participants attempting to outbid their peers to offer the best prices regardless of market supply and demand.

Through the conducted simulations, closer analysis reveals that the results of game-theoretic bidding strategies are sensitive to each agent's utility function as well as payoff determination method. Thus, detailed studies of consumer/prosumer behaviors can be conducted and modeled for future work. In addition, more complex ordering rules may be incorporated, such as prioritizing prosumers who generate higher quality of electricity or prioritizing low-income homeowners in need. Future work may also be expanded to include dynamic auction mechanisms where the smart contract adapts to varying supplies and demands in order to balance the P2P energy trading market. In addition, smart contracts and market clearing methods can be designed to account for physical network conditions and constraints through the incorporation of wheeling charges as an additional parameter of the game-theoretic bidding strategies. This work may also be further extended to support various DERs, alternative fuel exchanges, as well as other emerging economies.

References

- [1] Fu R, Feldman D, Margolis R. U.S. solar photovoltaic system cost benchmark: Q1 2018. National Renewable Energy Laboratory; 2018 [Online]. Available: <https://www.nrel.gov/docs/fy19osti/72399.pdf>. [Accessed: 28- Nov- 2018].
- [2] Form EIA-861M detailed data – Small Scale PV. Electricity, 2018. [Online]. Available: https://www.eia.gov/electricity/data/eia861m/xls/small_scale_solar_2018.xlsx. [Accessed: 04-Nov-2018].
- [3] Form EIA-861M detailed data – net metering. Electricity; 2018. [Online]. Available: https://www.eia.gov/electricity/data/eia861m/xls/net_metering2018.xlsx. [Accessed: 04-Nov-2018].
- [4] Boero R, Backhaus SN, Edwards BK. The microeconomics of residential photovoltaics: Tariffs, network operation and maintenance, and ancillary services in distribution-level electricity markets. *Sol Energy* 2016;140:188–98.
- [5] How many solar panels do you need to power your house?. Solar Power Rocks; 2018. [Online]. Available: <https://www.solarpowerrocks.com/square-feet-solar-roof/>. [Accessed: 28- Nov- 2018].
- [6] Consumers energy - experimental advanced renewable program. DSIRE; 2018. [Online]. Available: <http://programs.dsireusa.org/system/program/detail/5752>. [Accessed: 28- Nov- 2018].
- [7] November 2009. Electric power monthly; 2018. [Online]. Available: <https://www.eia.gov/electricity/monthly/archive/pdf/02260911.pdf>. [Accessed: 28- Nov- 2018].
- [8] Stokes LC, Breetz HL. Politics in the U.S. energy transition: Case studies of solar, wind, biofuels and electric vehicles policy. *Energy Policy* 2018;113:76–86.
- [9] Net metering. DSIRE; 2018. [Online]. Available: <http://programs.dsireusa.org/system/program/detail/342>. [Accessed: 28- Nov- 2018].
- [10] November 2018. Electric power monthly; 2018. [Online]. Available: https://www.eia.gov/electricity/monthly/epm_table_grapher.php?t=epmt_5_6_a. [Accessed: 25-Feb- 2019].
- [11] Electricity 2018. Wholesale electricity and natural gas market data; 2018. [Online]. Available: https://www.eia.gov/electricity/wholesale/xls/ice_electric-2018.xlsx. [Accessed: 25- Feb- 2019].
- [12] Rahimi FA, Ipkachchi A. Transactive energy techniques: closing the gap between wholesale and retail markets. *Electricity J* 2012;25(8):29–35.
- [13] Sousa T, Soares T, Pinson P, Moret F, Baroche T, Sorin E. Peer-to-peer and community-based markets: A comprehensive review. *Renew Sustain Energy Rev* 2019;104:367–78.
- [14] Tushar W, Yuen C, Mohsenian-Rad H, Saha T, Poor H, Wood K. Transforming energy networks via peer-to-peer energy trading: the potential of game-theoretic approaches. *IEEE Signal Process Mag* 2018;35(4):90–111 Available: 10.1109/msp.2018.2818327.
- [15] Zhang C, Wu J, Zhou Y, Cheng M, Long C. Peer-to-peer energy trading in a microgrid. *Appl Energy* 2018;220:1–12.
- [16] Andoni M, Robu V, Flynn D, Abram S, Geach D, Jenkins D, et al. Blockchain technology in the energy sector: A systematic review of challenges and opportunities. *Renew Sustain Energy Rev* 2019;100:143–74.
- [17] Henley C, Hartnett S, Endemann B, Tejblum B, Cohen DS. Energizing the future with Blockchain. *Energy Law J* 2018;39(2):197–232.
- [18] Brooklyn microgrid. Brooklyn Microgrid. [Online]. Available: <https://www.brooklyn.energy/>. [Accessed: 02- Sep- 2018].
- [19] New York consumers turn homes into connected power stations to take on the energy giants. LO3 Energy. [Online]. Available: <https://lo3energy.com/new-york-consumers-turn-homes-connected-power-stations-take-energy-giants/>. [Accessed: 02- Sep- 2018].
- [20] Mengelkamp E, Gärtner J, Rock K, Kessler S, Orsini L, Weinhardt C. Designing microgrid energy markets. *Appl Energy* 2018;210:870–80.
- [21] Latrobe valley microgrid feasibility study. Australian Renewable Energy Agency; 2018. [Online]. Available: <https://arena.gov.au/projects/latrobe-valley-microgrid-feasibility-study/>. [Accessed: 28- Nov- 2018].
- [22] Power ledger P2P platform goes across the meter with BCPG at T77 precinct, Bangkok. Medium; 2018. [Online]. Available: <https://medium.com/power-ledger/power-ledger-p2p-platform-goes-across-the-meter-with-bcpg-at-t77-precinct-bangkok-62df5aba3d0a>. [Accessed: 28- Nov- 2018].
- [23] Piclo energy. Piclo energy; 2018. [Online]. Available: <https://piclo.energy/>. [Accessed: 28- Nov- 2018].
- [24] Electron | blockchain systems for the energy sector. Electron; 2019. [Online]. Available: <http://www.electron.org.uk/>. [Accessed: 28- Nov- 2018].
- [25] SonnenCommunity. Sonnen Group; 2018. [Online]. Available: <https://sonnengroup.com/sonnencommunity/>. [Accessed: 28- Nov- 2018].
- [26] Electrify.Asia. Electrify.Asia; 2018. [Online]. Available: <https://electrify.asia/>. [Accessed: 28- Nov- 2018].
- [27] WePower. WePower; 2018. [Online]. Available: <https://wepower.network>. [Accessed: 28- Nov- 2018].
- [28] Enabling the open EV-economy of tomorrow. Share&Charge 2018. [Online]. Available: <https://shareandcharge.com/>. [Accessed: 28- Nov- 2018].
- [29] Liu N, Yu X, Wang C, et al. Energy-sharing model with price-based demand response for microgrids of peer-to-peer prosumers. *IEEE Trans Power Syst* 2017;32(5):3569–83.
- [30] Long C, Wu J, Zhang C, et al. Peer-to-peer energy trading in a community microgrid. In: Proc. of the 2017 IEEE power & energy society general meeting, 16-20 July 2017, Chicago, IL, USA.
- [31] Zhou Y, Wu J, Long C. Evaluation of peer-to-peer energy sharing mechanisms based on a multiagent simulation framework. *Appl Energy* 2018;222:993–1022. <https://doi.org/10.1016/j.apenergy.2018.02.089>.
- [32] Gregoratti D, Matamoros J. Distributed energy trading: The multiple-microgrid case. *IEEE Trans Ind Electron* 2015;62(4):2551–9.
- [33] Tushar Wayes, Saha Tapan, Yuen Chau, Morstyn Thomas, McCulloch Malcolm, Vincent Poor H, et al. A motivational game-theoretic approach for peer-to-peer energy trading in the smart grid. *Appl Energy* 2019;243. <https://doi.org/10.1016/j.apenergy.2019.03.111>.
- [34] Peer to peer energy trading with sustainable user participation: A game theoretic approach. *IEEE Access*, 2018; 6: 62932–43.
- [35] Calvillo C, Sánchez-Miralles A, Villar J, Martín F. Optimal planning and operation of aggregated distributed energy resources with market participation. *Appl Energy* 2016;182:340–57. <https://doi.org/10.1016/j.apenergy.2016.08.117>.
- [36] Faqiry M, Das S. Double-sided energy auction in microgrid: equilibrium under price anticipation. *IEEE Access* 2016;4:3794–805. <https://doi.org/10.1109/access.2016.2591912>.
- [37] El-Baz W, Tzscheutschler P, Wagner U. Integration of energy markets in microgrids: A double-sided auction with device-oriented bidding strategies. *Appl Energy* 2019;241:625–39. <https://doi.org/10.1016/j.apenergy.2019.02.049>.
- [38] Wang, Saad W, Han Z, Poor HV, Başar T. A game-theoretic approach to energy trading in the smart grid. *IEEE Trans. Smart Grid* 2014;5(3):1439–50.
- [39] Lee J, Gu JK, Choi, Zukerman M. Distributed energy trading in microgrids: A game-theoretic model and its equilibrium analysis. *IEEE Trans Ind Electron* 2015;62(6):3524–33.
- [40] Tushar W, Zhang JA, Smith DB, Poor HV, Thiebaux S. Prioritizing consumers in smart grid: A game theoretic approach. *IEEE Trans. Smart Grid* 2014;5(3):1429–38.
- [41] Case DM, Faqiry MN, Majumder BP, Das S, DeLoach SA. Implementation of a two-tier double auction for on-line power purchasing in the simulation of a distributed intelligent cyber-physical system. In: Espinoza FC, editor. Advances in artificial intelligence (research in computer science series), vol. 82; 2014. p. 79–91.
- [42] Luth A, Zepter JM, del Granado PC, Egging R. Local electricity market designs for peer-to-peer trading: the role of battery flexibility. *ApplEnergy* 2018;229:1233–43.
- [43] Long C, Wu J, Zhou Y, Jenkins N. Peer-to-peer energy sharing through a two-stage aggregated battery control in a community microgrid. *ApplEnergy* 2018;226:261–76.
- [44] Alam MR, St-Hilaire M, Kunz T. Peer-to-peer energy trading among smart homes. *Appl Energy* 2019;238:1434–43. <https://doi.org/10.1016/j.apenergy.2019.01.091>.
- [45] Market framework for local energy trading: A review of potential designs and

- market clearing approaches. IET Generation, Transmission & Distribution 2018; 12(22): p. 5899–908.
- [46] Babaioff M, Nisan N. Concurrent auctions across the supply chain. In: Proceedings of the 3rd ACM conference on Electronic Commerce - EC 01; 2001.
- [47] Parkes DC. Classic mechanism design. Available: www.eecs.harvard.edu/~parkes/pubs/ch2.pdf. [Accessed: 04-Sep-2018].
- [48] Satterthwaite MA, Williams SR. Bilateral trade with the sealed bid k-double auction: Existence and efficiency. *J Economic Theory* 1989;48(1):107–33.
- [49] Lin J, Pipattanasomporn M, Rahman S. Comparative analysis of blockchain- based smart contracts for solar electricity exchanges. 2019 IEEE power & energy society innovative smart grid technologies conference; 2019.
- [50] Feldman D, Margolis R. Q1/Q2 2018 solar industry update. National Renewable Energy Laboratory; 2018. [Online]. Available: <https://www.nrel.gov/docs/fy18osti/72036.pdf>. [Accessed: 28- Nov- 2018].
- [51] Olis D, Mosey G. Integration of rooftop photovoltaic systems in St. Paul Ford site's redevelopment plans. National Renewable Energy Laboratory 2015.
- [52] Commercial and residential hourly load profiles for all TMY3 locations in the United States. Open Energy Information. [Online]. Available: <https://openei.org/doe-opendata/dataset/commercial-and-residential-hourly-load-profiles-for-all-tmy3-locations-in-the-united-states>. [Accessed: 04-Sep-2018].
- [53] 5 Things to consider before you plan for a rooftop PV plant. Sustainability Outlook. [Online]. Available: <http://www.sustainabilityoutlook.in/content/5-things-consider-you-plan-rooftop-pv-plant>. [Accessed: 05-Sep-2018].
- [54] Typical roof pitch. MyRoof.com. [Online]. Available: <https://myrooff.com/standart-roof-pitch/>. [Accessed: 22-Nov-2018].